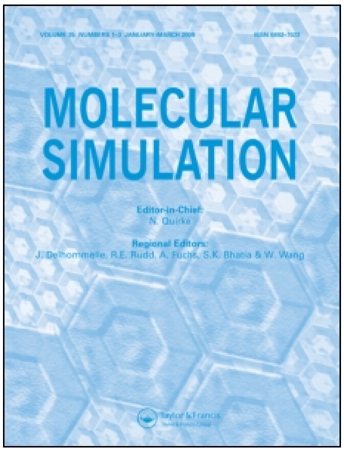

Molecular Simulation
Publication details, including instructions for authors and subscription information:
http://www.informaworld.com/smpp/title~content=t713644482

Differentiation of adenine non-planarity in valence molecular orbitals

M. T. Downton[a]; F. Wang[a]
[a] Centre for Molecular Simulation, Swinburne University of Technology, Victoria, Melbourne, Australia

To cite this Article Downton, M. T. and Wang, F.(2006) 'Differentiation of adenine non-planarity in valence molecular orbitals', Molecular Simulation, 32: 8, 667 — 673

To link to this Article: DOI: 10.1080/08927020600860911

URL: http://dx.doi.org/10.1080/08927020600860911

Molecular Simulation, Vol. 32, No. 8, 15 July 2006, 667–673

Differentiation of adenine non-planarity in valence molecular orbitals

M. T. DOWNTON*‡ and F. WANG¶

Centre for Molecular Simulation, Swinburne University of Technology, PO Box 218, Hawthorn, Melbourne, Victoria 3122, Australia

(Received November 2005; in final form December 2005)

Two molecular orbitals: MO7 (29*a*) and MO13 (23*a*) have been identified using dual space analysis (DSA) as the signatures of adenine non-planarity (C_1 point group symmetry). The non-planarity of adenine has been demonstrated to be from the attachment of the amino group (NH_2) to purine rings as well as the non-rigid deformability of the purine ring of adenine. Orbital 29*a* ($3a''$ in the planar case), a π-like orbital, is the direct result of the attachment of the amino group to the purine ring. Orbital 23*a* ($23a'$ in the planar case) is the result of the deformability of the purine ring in non-planar adenine (NP) and will be experimentally challenging to resolve.

Keywords: Adenine non-planarity; Dual space analysis; Valence molecular orbitals; Theoretical orbital momentum profiles

1. Introduction

The mechanisms of life are revealed when the molecular details are understood [1]. The nucleic acid bases adenine, guanine, cytosine and thymine represent some of the most important building blocks of life. Important and novel experimental and theoretical studies of the DNA bases can still be envisaged. One of the major outcomes of quantum–chemical studies of interaction of DNA bases was the discovery of the intrinsic non-planarity and high-flexibility of amino groups and their involvement in specific interactions in nucleic acids [2–5]. The situation was summarised by Hobza and Sponer when they stated: “clear, direct experimental evidence about the non-planarity of isolated bases is still missing due to the resolution of the available experimental techniques” [6]. This changed recently when Dong and Miller [7] used the vibrational transition moment angles (VTMA) technique to identify that the isolated adenine structure is a non-planar structure with the amino group (NH_2) out-of-plane by approximately 20°.

There exists extensive quantum mechanical (QM) molecular structural studies of the DNA bases including adenine. To be able to choose the appropriate method(s) and to eventually trust the predictive power of calculations, we need a thoughtful reconsideration of the computational work of the past. Some fundamental issues of adenine still constitute open questions. For example, although the non-planarity of the species has been studied [4,5,8–13] the majority of studies in DNA base structures do not focus on the molecular orbitals (MO), bonding mechanism, and the orbital consequence of planarity or non-planarity of adenine. The information obtained from coordinate space calculations is in general energy focused and can reveal little insight into chemical bonding mechanism and the changes of orbital shape in order to accommodate the non-planarity. The planar adenine (PA) and non-planar adenine (NP) structures do not have fundamental differences in isotropic properties, such as bond lengths and many other properties such as orbital energies, except for the out of plane position of the amino group and a degree of relaxation in the purine ring. This brings particular challenges to both theoretical and experimental studies unless novel methods and techniques which are sensitive to those properties can be identified or designed. Momentum space quantum chemistry applying dual space analysis (DSA) [14] can be a good candidate for this purpose. In this article, we report our most recent

---

*Corresponding author. Email: mdownton@sfu.ca

‡Current address: Department of Physics, Simon Fraser University, Burnaby, Canada, BC, V5A 1S6.

¶Email: fwang@swin.edu.au

Molecular Simulation
ISSN 0892-7022 print/ISSN 1029-0435 online © 2006 Taylor & Francis
http://www.tandf.co.uk/journals
DOI: 10.1080/08927020600860911

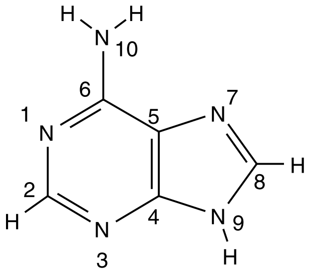

Figure 1. Adenine structure and its atomic numbering convention.

comparative study of PA and NP and identify the particular MO responsible for the structural relaxation of the species.

2. Method and computational details

DSA, which was introduced to study chemical bonding mechanisms of molecular systems in both coordinate and momentum space [14], is employed in this work. This method combines energy and other molecular properties obtained from conventional QM coordinate space with orbital momentum distributions (MDs) generated through a direct mapping of the wavefunctions into momentum space. It has been demonstrated [14–21] that DSA is a useful tool to study the chemical bonding mechanism of molecules, particularly isomers and tautomers, where there are minor energy differences between species. DSA makes full use of the strength of QM: the energetic properties in coordinate space differentiate orbitals on inequivalent sites in a molecule (e.g. the energy non-degenerate orbitals); whereas the momentum properties differentiate orbitals on (nearly) equivalent sites of a molecule (i.e. the energy degenerate or near degenerate orbitals) [21].

In this work the purine ring is in the *xy*-plane where the *y*-axis aligns parallel to the vector connecting $C_{(2)}$ and $N_{(1)}$ (figure 1). The model of B3LYP/TZVP has been employed to determine the geometries of PA (C_s symmetry) and NP (C_1 symmetry) isomers. The TZVP basis set is a reasonably large triple zeta with valence polarized (TZVP) basis set due to Godbout *et al.* [22]. This basis set has been particularly designed for DFT calculations and has been proved reliable in our previous work on adenine [17]. The computational chemistry GAMESS02 [23] suite of programs is employed in the present work. Separate single point calculations using RHF/TZVP, MP2/TZVP, B3LYP/TZVP as well as B3LYP/6-311++G** are then performed on optimised geometries obtained using the B3LYP/TZVP model. The molecular wavefunctions obtained from the single point calculations are mapped into momentum space (k-space) as orbital MDs, using the ground state configuration frozen (or independent particle) model and plane wave impulse approximation (PWIA) [24],

$$\sigma \propto \int d\Omega |\psi_j(\mathbf{k})|^2 \qquad (1)$$

which is proportional to the momentum space one-electron wavefunctions $\psi(\mathbf{k})$. It is the Fourier transform of one-electron wavefunction in coordinate space (r-space), known as Dyson orbitals, which are commonly approximated using the canonical HF or Kohn-Sham (KS) orbitals [25] under the ground state configuration frozen approximation (i.e. neglecting the ionic orbital relaxation). The orbital MDs, which are proportional to the orbital cross sections, can be measured by EMS experiments [26–31].

3. Results and discussion

3.1 Adenine geometry and properties in coordinate space

The B3LYP/TZVP model using the GAMESS-US02 program [23] gives the NP (X^1A) with C_1 point group symmetry a slightly lower total energy than the PA (X^1A') of C_s symmetry as shown in table 1. Although the energy difference between the PA and NP structures is small, the models at various levels consistently suggest a non-planar structure for adenine. Such an observation from the present work supports the claims that this DNA base ought to be considered as a "structurally nonrigid" species as found by other studies [5]. For example, Leszczynski *et al.* indicated that adenine possess high structural non-rigidity that manifests itself in the presence of normal ring out-ot-plane vibrations of NH_2 wag vibration of 158 cm^{-1} and the purine ring butterfly vibration of 207 cm^{-1} based on the MP2/6-31G** model [5].

The non-planarity of adenine does not lead to particular structural impacts on the geometry. In particular, the geometries of PA and NP based on the B3LYP/TZVP calculations do not exhibit significant different bond lengths. The PA atomic numbering system is same as the conventional system as indicated in figure 1. For NP and purine we therefore, adopt the same atomic numbering system as PA for comparison purposes. Table 2 gives the

Table 1. Ground state electronic energies of adenine: planar and non-planar (E_h)*.

Method	*Basis set*	*Planar (C_s)*	*Non-planar (C_1)*	$\Delta(E^{NP} - E^{P})$ *(eV)*
B3LYP	6−311++G**	−467.023943	−467.023947	−0.0001
B3LYP	TZVP	−467.408072	−467.408110	−0.0001
MP2	TZVP	−466.135160	−466.135809	−0.0177
RHF	TZVP	−464.622547	−464.622604	−0.0015

* GAMESS-US-02[23] was used.

Table 2. Geometries of PA and NP obtained using B3LYP/TZVP optimization*.

	Adenine (PA)	*Purine (PP)*	*Adenine (NP)*
Ring lengths/Å			
$\bar{R}_6$	8.162	8.147	8.163
$\bar{R}_5$	6.850	6.863	6.851
Angles/°			
$H_{(13)}-N_{(10)}-H_{(14)}$	120.266	–	119.732
$N_{(10)}-C_{(6)}-N_{(1)}$	119.093	–	118.933
$C_{(6)}-N_{(1)}-C_{(2)}$	118.590	118.270	118.630
$N_{(1)}-C_{(2)}-H_{(15)}$	115.387	116.113	115.357
$N_{(1)}-C_{(6)}-C_{(5)}$	118.542	119.862	118.610
$N_{(1)}-C_{(2)}-N_{(3)}$	128.516	127.672	128.571
$C_{(2)}-N_{(3)}-C_{(4)}$	111.433	112.422	111.391
$N_{(3)}-C_{(4)}-N_{(9)}$	128.757	129.112	128.719
$C_{(4)}-C_{(5)}-C_{(6)}$	126.589	125.872	126.626
$C_{(6)}-C_{(5)}-N_{(7)}$	132.463	133.474	132.568
$C_{(5)}-N_{(7)}-C_{(8)}$	104.314	104.398	104.299
$N_{(7)}-C_{(8)}-H_{(12)}$	125.403	125.132	125.321
$N_{(7)}-C_{(8)}-N_{(9)}$	113.055	113.676	113.164
$C_{(8)}-N_{(9)}-C_{(4)}$	106.702	106.287	106.691
$C_{(8)}-N_{(9)}-H_{(11)}$	127.554	127.584	127.348
Dihedral angles†/°			
$C_{(4)}-C_{(5)}-C_{(6)}-N_{(10)}$	–	–	178.992
$C_{(5)}-N_{(10)}-C_{(6)}-N_{(1)}$	–	–	179.155
$N_{(1)}-C_{(5)}-C_{(4)}-C_{(8)}$	–	–	179.614
$N_{(3)}-C_{(4)}-C_{(5)}-N_{(7)}$	–	–	−179.672
$C_{(4)}-C_{(5)}-N_{(7)}-C_{(8)}$	–	–	−0.091
$C_{(4)}-C_{(5)}-C_{(8)}-N_{(9)}$	–	–	−0.098
$N_{(7)}-N_{(9)}-C_{(4)}-C_{(5)}$	–	–	−0.092
$N_{(1)}-C_{(2)}-N_{(3)}-C_{(4)}$	–	–	−0.049
$C_{(2)}-C_{(6)}-C_{(5)}-C_{(4)}$	–	–	−0.033
$N_{(1)}-N_{(3)}-C_{(4)}-C_{(5)}$	–	–	0.112

*The geometry of purine in its ground electronic state (X^1A') is obtained using the same B3LYP/TZVP calculations as a reference. †The dihedral angles of PA and purine are either 180.0 or 0.0.

ring lengths, defined as the perimeters of the hexagon and pentagon rings of the purine rings [17] for PA, NP and purine. The changes in geometry between PA and NA are unnoticeable as the ring lengths are almost the exactly the same. However, the attachment of the amino group affects not only local atoms such as $C_{(6)}$ structurally, but also disturbs the planarity of the purine ring. As can be seen from table 2, the atoms in the purine rings of NP are not strictly in the same plane. The atom positions are relaxed and distorted from the planar symmetry to give a C_1 symmetry, that is, there is no molecular plane in NP adenine. However, only the non-planarity due to the amino group out of plane has been confirmed by experiment so far [7]. The purine ring distortion has been indicated theoretically [5]. Identifying such a subtle deformability in adenine will be an experimental challenge. The structural non-rigidity of this DNA base may have an impact on the DNA base interaction as well as the double helix structure, since most of the previous studies of nucleic acid bases were treated as rigid planar species [32].

It has been shown that energetic and some geometrical parameters are not sensitive enough to differentiate the PA and NP structures. The deformability of adenine has an angular dependency so that the dipole moments of the species are now examined. Dipole moment is obtained from the first derivative of the energy with respect to an applied electric field and provides a measure of the symmetry of the molecular charge distributions. The present B3LYP/TZVP calculations give the dipole moment (μ_x, μ_y and μ_z) of PA, NP and purine as (2.445, −0.045, 0.000), (2.440, −0.287, −0.085) and (2.784, 2.489, 0.000) Debye, respectively. Thus, the broken symmetry of NP can be seen from the non-zero z component of the dipole moment. Apart, from the small value of μ_z, there is however, little difference in the total moment for PA and NP (2.445 and 2.459 Debye, respectively). Both dipole moments are significantly different from the dipole moment of purine ($\mu = 3.734$ Debye), indicating that the attachment of the amino group to the purine ring has a significant impact on the electron charge distributions. Similar properties were found in our previous study of adenine tautomers [17]. As a result, the bonding mechanisms between adenine and purine can be quite different. However, this is out of the scope of the present work and will be discussed in detail elsewhere.

Table 3 gives the valence space MO and their energies for PA and NP in their ground states of X^1A' and X^1A, respectively, calculated using the RHF/TZVP//B3LYP/TZVP and B3LYP/TZVP//B3LYP/TZVP models. The valence orbital energies of adenine can be divided into two regions as outer valence region (MO1–15) and inner valence region (MO16–25). The energy difference between orbitals in the inner and outer valence regions is smaller, therefore, there is no a clear corder to separate these regions. It is also observed from this table, that the MOs with anti-symmetry a'', which indicates symmetric MOs with respect to the molecular plane, occur only in the outer valence region. Hence the π-bonds are formed in the outer valence region only, though this does not imply that there are no p-AOs participating in the inner valence and core regions of the species [15,16].

As the outer valence region possesses small orbital energy splittings, inclusion of electron correlation energy may alter the orbital energy ordering. This is seen in the PA case, that the symmetry alternation of the outer valence MO pairs of ($5a''$, $29a'$) and ($4a''$, $28a'$) between the RHF/TZVP//B3LYP/TZVP and B3LYP/TZVP//B3LYP/TZVP models. Finally, as indicated before, energy is not particularly sensitive to the non-planarity of adenine. The orbital energies using the same models of RHF/TZVP and B3LYP/TZVP, exhibit no fundamental differences between PA and NP. Hence, little insight into the non-planarity can be obtained from examination of table 3.

3.2 Orbitals correlated to adenine non-planarity in momentum space

The fact that the orbital energies of PA and NP are almost identical in coordinate space indicates that energy alone is insufficient in identifying the chemical bonding of NP. We therefore examined the orbital MDs of all MOs for planar and NP in the present work. Two orbitals of the NP, MO7 ($3a''$ for the PA and $29a$ for the NP) and MO13 ($23a'$ for the PA and $23a$ for the NP) can be identified as the orbitals responsible for the chemical bonding consequence of the

Table 3. Valence orbital energies and symmetries of adenine calculated using B3LYP/TZVP model chemistry (eV).

	Planar (C_s)			Non planar (C_1)		
	RHF/TZVP	B3LYP/TZVP		RHF/TZVP	B3LYP/TZVP	
MO	E	E	Sym.	E	E	Sym.
1*	−8.45	−6.21	$6a''$	−8.47	−6.22	35a
2	−10.16†	−6.98	$29a'$	−10.17	−6.99	34a
3	−11.15†	−7.43	$5a''$	−11.17	−7.44	33a
4	−11.55†	−7.89	$28a'$	−11.57	−7.89	32a
5	−12.28†	−8.20	$4a''$	−12.28	−8.21	31a
6	−13.48	−8.78	$27a'$	−13.47	−8.79	30a
7	−13.55	−9.86	$3a''$	−13.56	−9.87	29a
8	−15.19	−11.10	$2a''$	−15.19	−11.10	28a
9	−16.18	−11.58	$26a'$	−16.19	−11.58	27a
10	−16.81	−12.23	$25a'$	−16.80	−12.22	26a
11	−17.34	−12.65	$24a'$	−17.32	−12.65	25a
12	−17.35	−12.81	$1a''$	−17.38	−12.82	24a
13	−18.49	−13.75	$23a'$	−18.50	−13.75	23a
14	−19.06	−14.17	$22a'$	−19.05	−14.16	22a
15	−20.18	−15.16	$21a'$	−20.17	−15.15	21a
16	−21.28	−15.98	$20a'$	−21.28	−15.98	20a
17	−23.02	−17.24	$19a'$	−23.02	−17.24	19a
18	−23.91	−17.83	$18a'$	−23.92	−17.83	18a
19	−24.43	−18.27	$17a'$	−24.43	−18.28	17a
20	−28.21	−20.94	$16a'$	−28.22	−20.90	16a
21	−31.37	−23.45	$15a'$	−31.38	−23.46	15a
22	−32.31	−24.29	$14a'$	−32.32	−24.30	14a
23	−33.95	−25.57	$13a'$	−33.95	−25.58	13a
24	−35.40	−26.72	$12a'$	−35.41	−26.73	12a
25	−37.22	−28.30	$11a'$	−37.23	−28.31	11a

* The highest occupied molecular orbital (HOMO) of adenine. † The order of these MOs obtained from RHF/TZVP calculations is $5a''29a'4a''28a'$.

non-planarity of adenine. These two orbitals are both in the outer valence space, and are of a'' and a' symmetry for PA. As would be expected, the non-planarity of adenine as indicated by MO7 is associated with orbitals related to the amino group (NH_2), whereas MO13 is related to structural relaxation throughout the molecule.

The changes in MO7 are understandable as this MO has significant contributions from $N_{(10)}$, the nitrogen atom of the amino group and the non-planarity will reduce the orbital symmetry of a'', i.e. the molecular plane is no longer a nodal plane in NP. Figure 2 clearly indicates the orbital changes in momentum space from orbital MDs. In this figure, it is also clear that if it were planar, MO7 would have a nodal plane (figure 2 (ib)) and the π-like electron charge distributions (the wire plot, Figure 2 (ia)) would be symmetric with respect to the molecular plane. However, in the case of NP, there does not exist a nodal plane for the orbital. The amino group and other atoms in the hexagon-ring to which the amino group attached are populated, whereas the pentagon ring has negligible influence in the orbital (figure 2 (iib)). Therefore, MO7 can be considered as the evidence of the non-planarity of adenine caused by the amino group.

Figure 3 gives the other orbital, MO13, as identified by the orbital MDs. However, it is quite surprising that this orbital has an a' symmetry rather than an a'' symmetry in the PA case. The orbital electron charge density (figure 3 (ib) and (iib)) in the planar and NP indicates that this orbital receives contributions from all atoms in a delocalised σ fashion, that is, there is no nodal plane in these cases and the orbital resides in the plane. The orbital MDs indicate that the orbital in PA and NP are slightly different in the long range, low momentum region. The orbital charge distribution (wire plots) clearly indicates the planarity. Figure 3 (ia) exhibits the overlapped wires, whereas figure 3 (iia) displays slightly blurred wires for the NP orbital. Apparently, this orbital is not responsible for the non-planarity of adenine due to the amino group. As indicated in table 2, the dihedral angles of the atoms in the hexagon-ring and pentagon-ring in the NP case do show the non-planarity. For example, the dihedral angles of $N_{(1)}–C_{(5)}–C_{(4)}–C_{(8)}$, $N_{(3)}–C_{(4)}–C_{(5)}–N_{(7)}$, $N_{(7)}–N_{(9)}–C_{(4)}–C_{(5)}$ and $N_{(1)}–N_{(3)}–C_{(4)}–C_{(5)}$ of NP are 179.614 and −179.672°, −0.092 and 0.112°, respectively, whereas those angles in PA and purine are either 180 or 0° accordingly. As a result, this orbital, MO13 (29a) can be considered as the signature of the deformability of the purine ring in NP.

4. Conclusions

The present work using DSA has indicated that PA and NP structures could coexist with almost negligible lower energy to prefer non-planarity. However, it is certainly possible to identify the MO which are directly associated

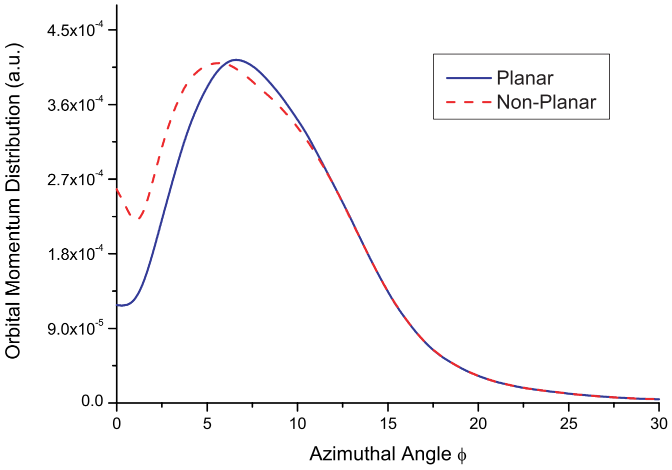

(ia) MO7 (planar adenine, 3a")

(ib) MO7 (planar adenine (nodal plane), 3a")

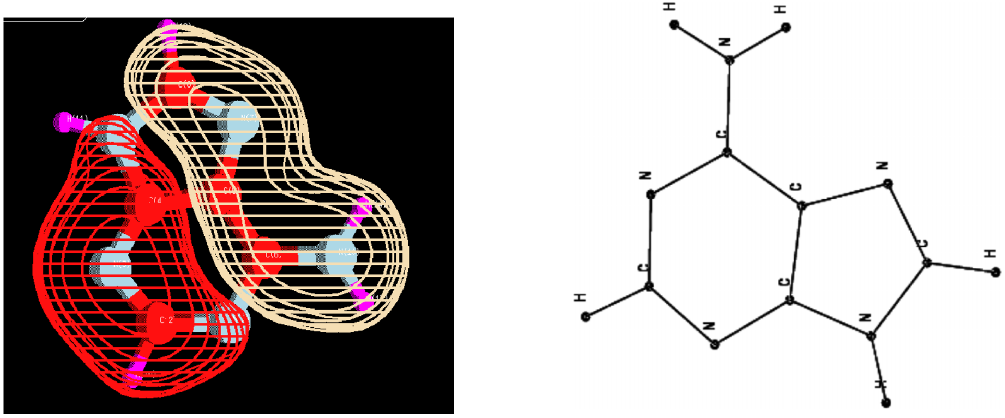

(iia) MO7 (non-planar adenine, 29a)

(iib) MO7 (non-planar adenine, 29a)

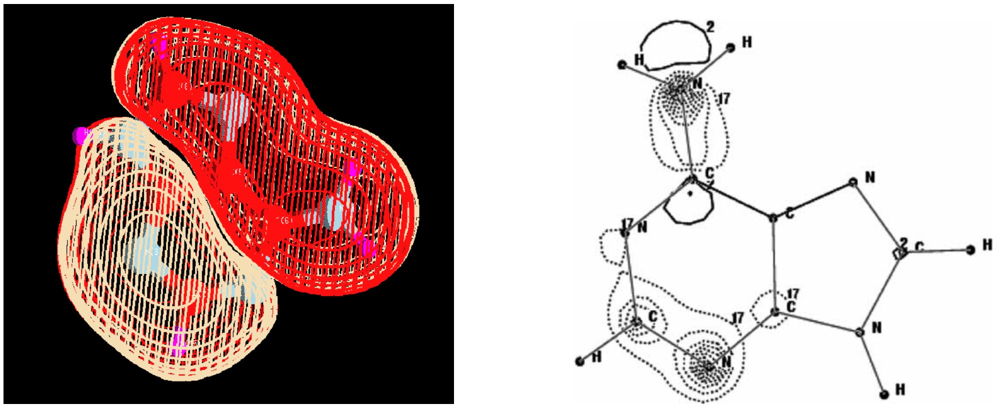

Figure 2. Orbital 7—the amino group signature: the most apparent differences in MOs due to planar (3a″) and non-planar (29*a*) adenine generated by the B3LYP/TZVP//B3LYP/TZVP model. The orbital charge densities are plotted using molden [33].

with the non-planarity of adenine. As expected, molecular orbital MO7 (29*a*), a π-like orbital which directly link with the attachment of the amino group, exhibits the non-planarity by splitting orbital MDs from the PA orbital. It is found that the attachment of the amino group (NH) is not a local effect but significantly contributes to the electron charge redistribution of the purine ring planarity. The delocalised σ-like MO13 (23*a*) reflects the deformability of the purine ring in NP. In conclusion, adenine non-planarity is not solely due to the amino ring out of plane

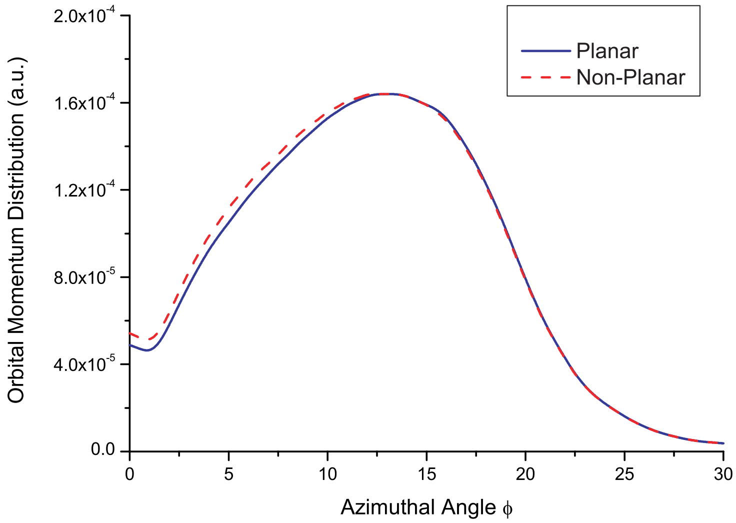

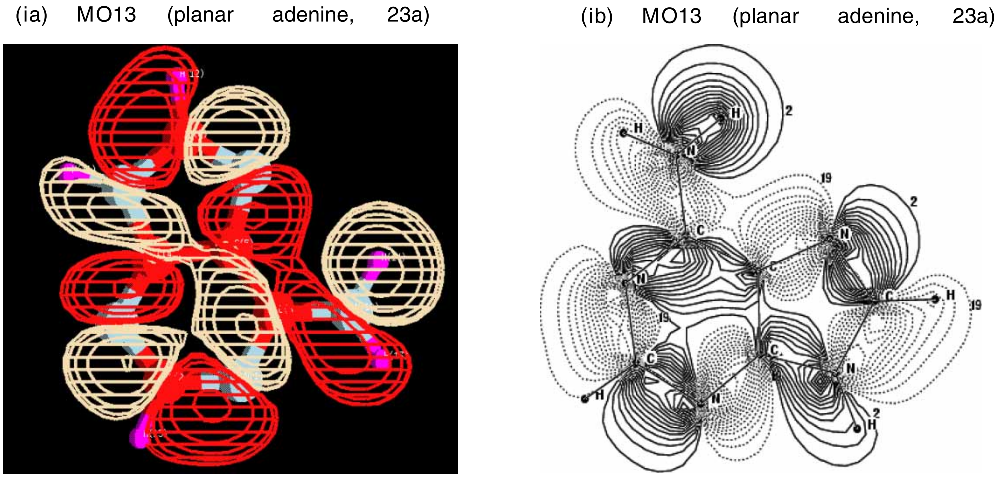
(ia) MO13 (planar adenine, 23a)

(ib) MO13 (planar adenine, 23a)

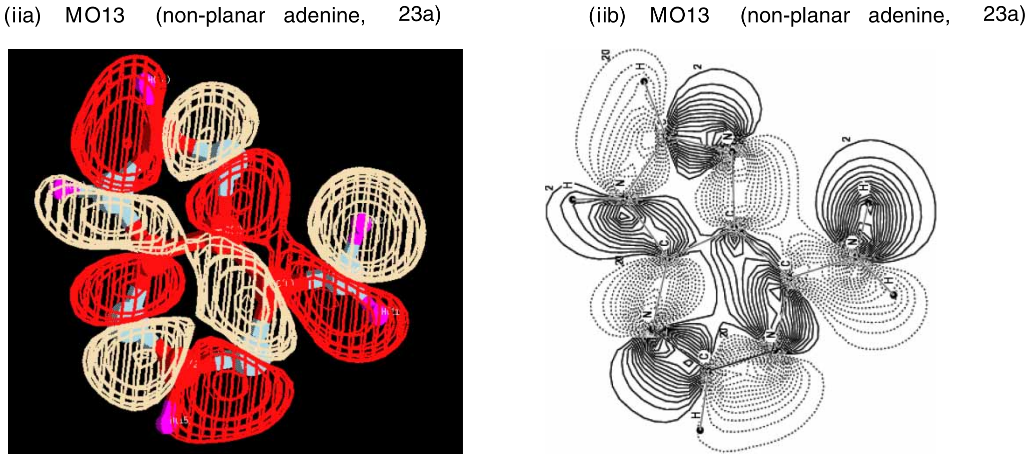
(iia) MO13 (non-planar adenine, 23a)

(iib) MO13 (non-planar adenine, 23a)

Figure 3. Orbital 13—the signature of purine ring deformability: the observable differences in MOs due to planar ($23a'$) and non-planar ($23a$) adenine generated by the B3LYP/TZVP//B3LYP/TZVP model. The orbital charge densities are plotted using molden [33].

contributions, but also from the non-planarity of the purine ring. The former has been directly confirmed by experiment but a direct experimental confirmation of the latter will be a challenge.

Acknowledgements

This work is supported by the Australian Research Council (ARC) and by Swinburne University of

Technology Vice-Chancellor's Strategic Research Initiative Grant. The authors acknowledge the Australian Partnership for Advanced Computing (APAC) for use of the National Supercomputing Facilities.

References

[1] The National Academies Press. *Board On Chemical Sciences and Technology, National Research Council, Beyond the Molecular Frontier: Challenges For Chemistry and Chemical Engineering*, The National Academies Press, Washington, DC (2003).

[2] J. Sponer, P. Hobza. Molecular interactions of nucleic acid bases. A review of quantum–chemical studies. *Collect. Czech. Chem. Commun.*, **68**, 2231 (2003).

[3] J. Leszczynski. Are the amino-groups in the nucleic-acid bases coplanar with the molecular rings? *Ab initio* HF/6-31G* and MP2/6-31G* studies. *Int. J. Quant. Chem., Suppl.*, **19**, 43 (1992).

[4] J. Sponer, P. Hobza. Nonplanar geometries of DNA bases—*ab initio* 2nd-order Moller-Plesset study. *J. Phys. Chem.*, **98**, 3161 (1994).

[5] O.V. Shishkin, L. Gorb, P. Hobza, J. Leszczynski. Structural nonrigidity of nucleic acid bases. Post-Hartree-Fock *ab initio* study. *Int. J. Quant. Chem.*, **80**, 1116 (2000).

[6] P. Hobza, J. Sponer. Structure, energetics, and dynamics of the nucleic acid base pairs: Nonempirical *ab initio* calculations. *Chem. Rev.*, **99**, 3247 (1999).

[7] F. Dong, R.E. Miller. Vibrational transition moment angles in isolated biomolecules: A structural tool. *Science*, **298**, 1227 (2002).

[8] J. Leszcynski. Electron correlation effects in the *ab initio* study on tautomerism of guanine. *Chem. Phys. Lett.*, **174**, 347 (1990).

[9] N.V. Riggs. An *ab initio* study of the stationary structures of the major gas-phase tautomer of adenine. *Chem. Phys. Lett.*, **177**, 447 (1991).

[10] N. Kurita, V.I. Danilov, V.M. Anisimov. The structure of Watson-Crick DNA base pairs obtained by MP2 optimization. *Chem. Phys. Lett.*, **404**, 164 (2005).

[11] M.J. Nowak, L. Lapinski, J. Fulara, A. Les, L. Adamowicz. Matrix-isolation IR spectroscopy of tautomeric systems and its theoretical interpretation—2-hydroxypyridin/2(1H)-pyridinone. *J. Phys. Chem.*, **96**, 1562 (1992).

[12] O. Bludsky, J. Sponer, J. Leszczynski, V. Spirko, P. Hobza. Amino groups in nucleic acid bases, aniline, aminopyridines, and aminotriazine are nonplanar: Results of correlated *ab initio* quantum chemical calculations and anharmonic analysis of the aniline inversion motion. *J. Chem. Phys.*, **105**, 11042 (1996).

[13] J. Sponer, J. Florian, P. Hobza, J. Leszczynski. Nonplanar DNA base pairs. *J. Biomol. Struct. Dyn.*, **13**, 827 (1996).

[14] F. Wang. Assessment of quantum mechanical models based on resolved orbital momentum distributions of *n*-butane in the outer valence shell. *J. Phys. Chem. A*, **107**, 10199 (2003).

[15] F. Wang, M. Downton. Inner valence shell bonding mechanism of *n*-butane studied using orbital momentum distributions of its conformational isomers. *J. Phys. B: At. Mol. Opt. Phys.*, **37**, 557 (2004).

[16] M. Downton, F. Wang. Chemical bonding mechanisms of *n*-butane probed by the core orbitals of conformational isomers in r-space and k-space. *Chem. Phys. Lett.*, **384**, 144 (2004).

[17] F. Wang, M.T. Downton, N. Kidwani. Adenine tautomer electronic structural signatures studied using dual space analysis. *J. Theo. Comp. Chem.*, **4**, 247 (2005).

[18] S. Saha, F. Wang, C.T. Falzon, M.J. Brunger. Coexistence of 1,3-butadiene conformers in ionization energies and Dyson orbitals. *J. Chem. Phys.*, **123**, 124315 (2005).

[19] C.T. Falzon, F. Wang. Understanding glycine conformation through molecular orbitals. *J. Chem. Phys.*, **123**, 214307 (2005).

[20] S. Knippenberg, K.L. Nixon, H. Mackenzie-Ross, M.J. Brunger, F. Wang, M.S. Deleuze, J.P. Francois, D.A. Winkler. Investigation into the valence electronic structure of norbornene using electron momentum spectroscopy, Green's function, and density functional theories. *J. Phys. Chem. A*, **109**, 9324 (2005).

[21] F. Wang. The electronic structural information from core orbitals of norbornadiene, norbonene and norbornane. *J. Mol. Struct. THEOCHEM.*, **728**, 31 (2005).

[22] N. Godbout, D.R. Salahub, J. Andzelm, E. Wimmer. Optimization of Gaussian-type basis-sets for local spin-density functional calculations .1. Boron through neon, optimization technique and validation. *Can. J. Chem.*, **70**, 560 (1992).

[23] M.W. Schmidt, K.K. Baldridge, J.A. Boatz, S.T. Elbert, M.S. Gordon, J.H. Jensen, S. Koseki, N. Matsunaga, K.A. Nguyen, S.J. Su, T.L. Windus, M. Dupuis, J.A. Montgomery. General atomic and molecular electronic-structure system. *J. Comp. Chem.*, **14**, 1347 (1993).

[24] E. Weigold, I. McCarthy. *Electron Momentum Spectroscopy*, Kluwer Academic/Plenum Publishers, New York (1999).

[25] P. Duffy, D.P. Chong, M.E. Casida, D.R. Salahum. Assessment of KS density-functional orbitals as approximate Dyson orbitals for the calculation of electron-momentum-spectroscopy scattering cross-sections. *Phys. Rev. A*, **50**, 4707 (1994).

[26] S. Knippenberg, K.L. Nixon, M.J. Brunger, T. Maddern, L. Campbell, N. Trout, F. Wang, W.R. Newell, M.S. Deleuze, J.P. Francois, D.A. Winkler. Norbornane: An investigation into its valence electronic structure using electron momentum spectroscopy, and density functional and Green's function theories. *J. Chem. Phys.*, **121**, 10525 (2004).

[27] K.L. Nixon, F. Wang, L. Campbell, T. Maddern, D. Winkler, R. Gleiter, P. Loeb, E. Weigold, M.J. Brunger. An electron momentum spectroscopy and density functional theory study of the outer valence electronic structure of stella-2,6-dione. *J. Phys. B.: At. Mol. Opt. Phys.*, **36**, 3155 (2003).

[28] S.A.C. Clark, T.J. Reddish, C.E. Brion, E.R. Davidson, R.F. Frey. The valence orbital momentum distributions and binding energy spectra of methane by electron momentum spectroscopy—quantitative comparisons using near Hartree-Fock limit and correlated wave-functions. *Chem. Phys.*, **143**, 1 (1990).

[29] F. Wang, H. Mackenzie-Ross, D.A. Winkler, I.E. McCarthy, L. Campbell, M.J. Brunger. A high-resolution electron momentum spectroscopy and density functional theory study into the complete valence electronic structure of allene. *J. Comp. Chem.*, **22**, 1321 (2001).

[30] Y. Zheng, J.J. Neville, C.E. Brion. Imaging the electron-density in the highest occupied molecular-orbital of glycine. *Science*, **270**, 786 (1995).

[31] J.J. Neville, Y. Zheng, C.E. Brion. Glycine valence orbital electron densities: Comparison of electron momentum spectroscopy experiments with Hartree-Fock and density functional theories. *J. Am. Chem. Soc.*, **118**, 10533 (1996).

[32] W. Saenger. *Principles of Nucleic Acid Structure*, Springer, New York (1988).

[33] G. Schaftenaar, J.H. Noordik. Molden: a pre- and post-processing program for molecular and electronic structures. *J. Comput. Aided Mol. Des.*, **14**, 123 (2000).